infrastructures

MDPI

Article

Flexible Permeable-Pavement System Sustainability: A Methodology for Stormwater Management Based on PM Granulometry

Vittorio Ranieri [1,*], Stefano Coropulis [1], Veronica Fedele [1], Paolo Intini [2] and John Joseph Sansalone [3]

[1] Department of Civil, Environmental, Land, Construction and Chemistry, Politecnico di Bari, 70126 Bari, BA, Italy; stefano.coropulis@poliba.it (S.C.); veronica.fedele@poliba.it (V.F.)
[2] Department of Innovation Engineering, Università del Salento, 73047 Lecce, LE, Italy; paolo.intini@unisalento.it
[3] Engineering School of Sustainable Infrastructure and Environment (ESSIE), University of Florida, Gainesville, FL 32611, USA; jsansal@ufl.edu
* Correspondence: vittorio.ranieri@poliba.it; Tel.: +39-0805963413

Abstract: Permeable-pavement design methodologies can improve the hydrologic and therefore the environmental benefits of rural and urban roadway systems. By contrast, conventional impervious pavements perturb the hydrologic cycle, altering the relationship between the rainfall loading and runoff response. Impervious pavements create a hydraulically conductive interface for the transport of traffic-generated chemicals and particulate matter (PM), deleteriously impacting their proximate environments. Permeable-pavement systems are countermeasures to mitigate hydrologic, chemical, and PM impacts. However, permeable pavements are not always equally implementable due to costs, PM loadings, and design constraints. A potential solution to facilitate environmental benefits while meeting the traffic load capacity is the combination of two filtration systems placed at the pavement shoulders and/or pedestrian sidewalks: a bituminous-pavement open-graded friction course (BPFC) and an aggregate-filled infiltration trench. This solution is presented in this manuscript together with the methodological framework and the first results of the investigations into designing and validating such a combined system. The research was conducted at the laboratories of the Polytechnic University of Bari and the University of Florida, while an operational and full-scale physical model was constructed in Bari, Italy. The first results presented characterize the PM deposition on public roads based on granulometry (particle size distributions (PSDs) and particle number densities (PNDs)). Samples (n = 16) were collected and analyzed at eight different sites with different land uses, traffic, and pavements from different cities (Bari and Taranto, Italy). The PM analysis showed similar distributions (PSDs and PNDs), except for two samples. The gravimetric-based PSDs of the PM had granulometric distributions in the sand-size range. In contrast, the PNDs, modeled by a Power Law Model (PLM) ($R^2 \geq 0.92$), illustrated an exponentially increasing number of particles in the fine silt and clay-size range, representing less than 10% of the PSD mass. Moreover, the results indicate that PM sourced from permeable-pavement systems has differing impacts on the pavement service life.

Keywords: sustainable; flexible pavement; bituminous-pavement open-graded friction course; roadway PM; particle size distribution; particle number density; material properties

Citation: Ranieri, V.; Coropulis, S.; Fedele, V.; Intini, P.; Sansalone, J.J. Flexible Permeable-Pavement System Sustainability: A Methodology for Stormwater Management Based on PM Granulometry. *Infrastructures* **2024**, *9*, 95. https://doi.org/10.3390/infrastructures9060095

Academic Editors: Giuseppe Cantisani and Giulia Del Serrone

Received: 16 April 2024
Revised: 4 June 2024
Accepted: 7 June 2024
Published: 11 June 2024

1. Introduction

Currently, approximately 55% of the world population lives in urban areas, and, according to estimates, this proportion will increase up to 65% by 2050 [1]. The increasing demographic trend in urbanization has led to significant expanses of impervious surfaces. A primary consequence of this trend is the reduction in the permeable interface between the atmosphere and soil, resulting in deleterious environmental and public health consequences [2]. Therefore, urbanization with the commensurate implementation of impervious

pavement surfaces poses challenges for sustainable development, the hydrologic cycle, the environment, and public health. The implementation of policies and designs aimed at promoting and supporting new and sustainable frameworks of infrastructure development is therefore necessary [3].

The sustainability of roadway infrastructure is uniquely challenging for urban and rural areas. While these areas have disparate population densities [4,5], urban areas, to a larger degree, are impacted deleteriously by chemical, PM, traffic noise [6], and thermal loads [5]. In this context, pavement systems have a significant impact across built environs, since such pavement systems are conventionally constructed of impervious materials and densified/compacted soils [7,8]. Roads interrupt the natural hydrologic processes of the storage–infiltration–evaporation of the vegetated soil surface, altering the environmental equilibrium between the rainfall and runoff [9,10], chemistry and chemical, and PM loads transported in the runoff (stormwater) [11]. In contrast to concrete pavements, large expanses of bituminous impervious pavements increase surface and near-surface temperatures [8,12], contributing to the urban heat island (UHI) phenomenon [8,12,13]. Moreover, impervious surfaces represent a primary source for loads of dry accretion of hetero-dispersed traffic-generated PM [14,15] and chemicals, including metals, plastics, and organics [16], during inter-event dry periods. Additionally, the vehicular traffic associated with a rainfall–runoff event (vehicles during storm (VDSs)) represents a significant source and vector for PM and chemical loads [17,18]. If the runoff is not well managed through methodologies to sequester the PM and reduce the chemical-load transport [19], the runoff and loads conveyed from pavement surfaces will have environmental impacts on the receiving waters and soils.

To manage runoff, PM, and chemical loads, the combination of an infrastructure system that presents a permeable pavement (e.g., bituminous-pavement open-graded friction course (BPFC)) draining to a volumetric infiltration unit as an adjuvant for load sequestration is an alternative design to impervious pavement systems. Permeable pavements are designed for roadway infrastructure, function as conventional road pavement infrastructure for vehicular transport, and consist of open-graded asphalt or permeable concrete. Variations of such infrastructure are permeable asphalt systems (PASs) (commonly known in Europe as porous asphalt) and concrete permeable pavement (CPP). These permeable infrastructure components can provide passive hydrologic, PM, and chemical mitigation as the primary unit in a multi-component infrastructure system. Furthermore, permeable pavements mitigate UHI impacts and reduce traffic noise [13,20], and they improve safety through increased skid resistance [20]. Beyond the mitigation of the rainfall–runoff load response [20,21], mechanistic phenomena for passively managing PM and chemical loads are facilitated by adsorption–filtration unit operations and processes. The aggregate granular matrix of such a multi-component infrastructure system provides alkalinity and hardness (Ca and Mg) to mitigate metal toxicity [22,23], especially when combined with engineered exfiltration granular layers [24,25].

Permeable-pavement variants such as PASs are deployed for highways [26] in areas where the asphalt pavements are commonly specified based on construction practice experience and conventions. PASs intended as full-depth permeable structures provide in situ unit process mechanisms to passively sequester chemicals in runoff, yielding environmental advantages [27] and the mitigation of the UHI [28]. In contrast to CPP, PASs provide lower buffering alkalinity/hardness and therefore less surface complexation (ion-exchange and chemical-precipitation mechanisms) potential for chemical sequestration [13]. As for the unit operation mechanisms, predominately filtration, PASs can have similar PM filtration and chemical-load sequestration efficiencies to those of CPP variants of equivalent pore size distributions and depths (thicknesses) [26]. However, installing a full-depth PAS or CPP is not always possible due to the specific constraints (for instance, based on a lower subgrade bearing capacity). For this reason, these systems have historically been implemented for surface parking systems in which the traffic loads are low, and these systems can also have mitigating effects for temperature and moisture transport [13]. For roads where the

required bearing capacity due to traffic is high, a potentially more viable alternative to PASs and CPP is a BPFC as a renewable wearing surface layer of the pavement system. With the goal of sustainability and material reuse in a circular economy, other forms of pavements can provide high bearing capacities, such as microwave-heated asphalt concrete with functional aggregates and waste ferrite [29], coal gangue [30], or fillers [31]. Despite the benefits introduced by these asphalt pavements, BPFCs also provide stormwater management. The thickness of the BPFC is limited to the upper centimeters of the pavement for bearing-capacity purposes [26], while still ensuring that it provides stormwater management functionality. This functionality includes infiltration, some level of detention storage and pore space residence time (RT), as well as tortuous filtration based on the drainage gradient and pore size distribution of the BPFC [32,33]. Drainage gradient and pore size design considerations mitigate the flow pore velocity to provide a sufficient RT and residence time distribution (RTD), as an index of short circuiting and preferential flow, within the BPFC to reduce the potential deterioration of the bonds between the asphalt and aggregates. The erosive action of preferential flow can create micro-sized cracks that progress to macro-sized cracks, leading to the structural damage of the BPFC subject to vehicular loads. Gradient and pore size distribution considerations can mitigate these phenomena and are a major consideration when considering the filtration capacity and maintenance cycle to recover the PM filtrate from the BPFC. Apart from the permeable upper layer, all the other layers of this pavement system are traditional to ensure adequate mechanical strength. With respect to runoff management, even though the BPFC can mitigate the runoff characteristics of a rainfall event, the hydrologic/hydraulic performance may differ (depending on the interflow path and length) from a full-depth PAS or CPP. Since one consideration for the application of permeable-pavement systems is stormwater reuse, the BPFC and maintenance thereof should manage the chemicals, PM, and organics, such as oil and grease, within the thresholds defined by the relevant standards.

While the BPFC provides a primary treatment function, the discharge (as primary effluent) can be directed to a secondary treatment system to obtain the same or higher treatment function as those of PASs and CPP. In the literature, there are permeable pavements that combine filtration layers in order to improve their efficiency [34–39]. In some cases, the PM reduction for runoff can approach or exceed 90% [23]. In one example, the mean sequestration of PM, after a rainfall simulation of 35 years, was approximately 92% [40]. However, the PM retained in the permeable matrix does correlate to the clogging of the pavement. In fact, it was demonstrated that the highest percentage of retention happened in the upper layer of the pavement, where the porosity was the highest. After five years, clogging (PM sequestration in the upper-pavement porosity) decreased the hydrologic/hydraulic performance [41–43]. This phenomenon can be avoided by means of common cleaning and maintenance procedures at more frequent intervals [44].

The combination of permeable systems (e.g., BPFCs) increases the treatment performance of permeable-pavement systems and helps mitigate the clogging potential in the pavement surface pores that can be more readily managed by cleaning. From this consideration, this study illustrates a permeable system made of a BPFC wearing surface combined with an aggregate (AGG) infiltration trench placed at the shoulders and/or sidewalks (where runoff is transported), to achieve or exceed the performance of CPP and full-depth PASs. This paper presents the studies for developing such a proposed system. As part of a wide research program, here, the general purposes and methodology are presented together with the initial results of the material characterization.

This comprehensive study for the design and validation of this system required several steps, which are summarized in the following list:

- Statement of the problem, overall set-up of the experimental work;
- Characterization of permeable-system material properties [45];
- Characterization of PM [46];
- Laboratory evaluation of the system efficiency;
- Field evaluation and validation of the system;

- Temporal monitoring of the system efficiency.

The study work was conducted in the laboratories of the Polytechnic University of Bari and the University of Florida. An operational full-scale physical model was also constructed in Bari, Italy.

Considering these aspects, the first objective of the manuscript is to define the concept of a flexible permeable-pavement combined system for runoff management and treatment (filtration). With the analysis of the materials involved in the permeable-pavement system, the second objective is characterizing the PM granulometry that loads the system and therefore requires passive management through filtration by the system. The third objective is the collection and subsequent characterization of the PM collected on roads through the determination of the particle size distribution (PSD) and particle number density (PND) indices. This third objective, while rarely carried out, provides valuable insights into the design and management of such systems.

The remainder of the paper is organized as follows. The "Materials and methods" Section summarizes the materials investigated for the research program, before focusing on the materials and procedures used for the initial material characterization. Subsequently, the results coming from the application of the first steps of the physical model are presented and discussed. The main conclusions from this study are drawn in the final section.

2. Materials and Methods

Characterizing the BPFC+AGG as a potentially sustainable system requires an investigation for obtaining reliable and reproducible results. The main goal of the proposed design is to find the balance between PM filtration for the stormwater management, safety, and good mechanical performance of the system [47–49]. As for the mechanical performance, design procedures for permeable pavement have already been developed [50], as well as for the hydraulic performances of CPP [51,52] and PASs [50,53]. However, a comprehensive analysis of the environmental efficiency of the BPFC+AGG permeable system is still lacking, and the physical model configuration is shown in this section.

2.1. Materials

The proposed flexible permeable-pavement combined system for stormwater management is composed of two main elements:

- A bituminous-pavement open-graded friction course (BPFC);
- An infiltration trench made of natural aggregates (AGGs).

During a runoff event, the system works "in series": the influent source area pavement runoff infiltrates through the BPFC with a combination of vertical and then horizontal transport and is then transported into the secondary infiltration trench providing vertical filtration. Thus, the primary infrastructure components/materials characterized are as follows:

1. The BPFC: Hydraulic conductivity tests are required to understand the response to runoff loadings. Variations in hydraulic conductivity testing can be implemented according to the realistic flow path of the water within the porous structure. Moreover, the porosity can be reduced over time due to the pavement geometrics (such as the pavement gradient) and the progression of filter ripening that alters the hydraulic (RT and RTD) and filtration capacity of the BPFC structure. For this reason, the BPFC response to clogging is required;
2. The infiltration trench made of natural aggregates (AGGs): This system must also be tested with respect to its hydraulic conductivity to determine the hydraulic response (RT and RTD). Considering that AGGs can have an effective porosity greater than the BPFC, the AGG hydraulic conductivity will be greater than that of the BPFC, and that the predominant flow path and direction through this structure will be different. In the case of AGGs, the flow is mostly vertical, rather than horizontal. The clogging determination is considered secondary for the AGG system, given that the BPFC is the

primary filtration unit, and the AGGs are not only the secondary unit but also show their high effective porosity. Therefore, the AGGs will have a lower clogging potential and longer maintenance interval, since the BPFC alters the PSD and concentration of PM as the primary effluent discharging into the AGGs;

3. Particulate matter (PM): The filtration capabilities of the BPFC+AGG system are directly impacted by the PM granulometry, source area influent hydraulic loads notwithstanding. Quantifying the PM granulometry is crucial to quantifying the system response. The PM loading is a primary consideration; thus, this was the first aspect of the investigation. The PM characterization is detailed in the next sections.

2.2. Siting of the Full-Scale Physical Model

The full-scale physical model was installed at the Adriatico Bridge. The bridge, as shown in Figure 1a, was constructed in Bari, Apulia, Italy, in 2016. The full-scale physical model is shown in the foreground of Figure 1b.

Figure 1. (**a**) Lateral view of Adriatico Bridge (source: cimolai.com, last accessed on the 31 October 2023) and (**b**) picture from the full-scale physical model system construction.

As previously mentioned, the road infrastructure is paved with a BPFC as a component of the integrated drainage pavement system for the bridge. The water, after passing through the BPFC, is hydraulically transmitted by gravity into the AGG trench that is located under the sidewalk, as part of the integrated drainage system. After this secondary treatment, the water passes into an inspection chamber of pipes and is released into the urban sewerage combined (wet- and dry-weather flow) system. In the control station of the full-scale physical model, samples can be collected to measure the PM and chemicals in the treated secondary effluent before they are discharged to the public combined sewer system.

The system covers a longitudinal section of 60 m, and it is located at the northern end of the bridge, on the shoulder placed on the east side. The physical-model system is composed of two unit operations (UOs) from a water treatment perspective:

- The BPFC, the roadway wearing surface with a thickness of 5 cm, is the primary UO. The areal extension is 60 m × 8 m (length × width). The BPFC is characterized by a 19% porosity, a percentage of bitumen of 5.3%, a maximum aggregate diameter (D_{max}) equal to 14 mm, and a d_{50} equal to 7 mm. The Marshall stiffness modulus was greater than 150 daN/mm, according to the standard design sheet of the project;
- The infiltration trench (AGGs) is the secondary UO and is partly placed under the shoulder of the road pavement and partly under the sidewalk, for the whole length of the physical-model geometry extent. The infiltration trench is filled with coarse stone aggregates made of limestone (d_{50} = 5.92 mm), providing alkalinity and hardness to the treated runoff. A micro-slotted pipe is placed on the bottom of the system for the collection of filtered water. This system is parallel to the sewerage system shown in Figure 2.

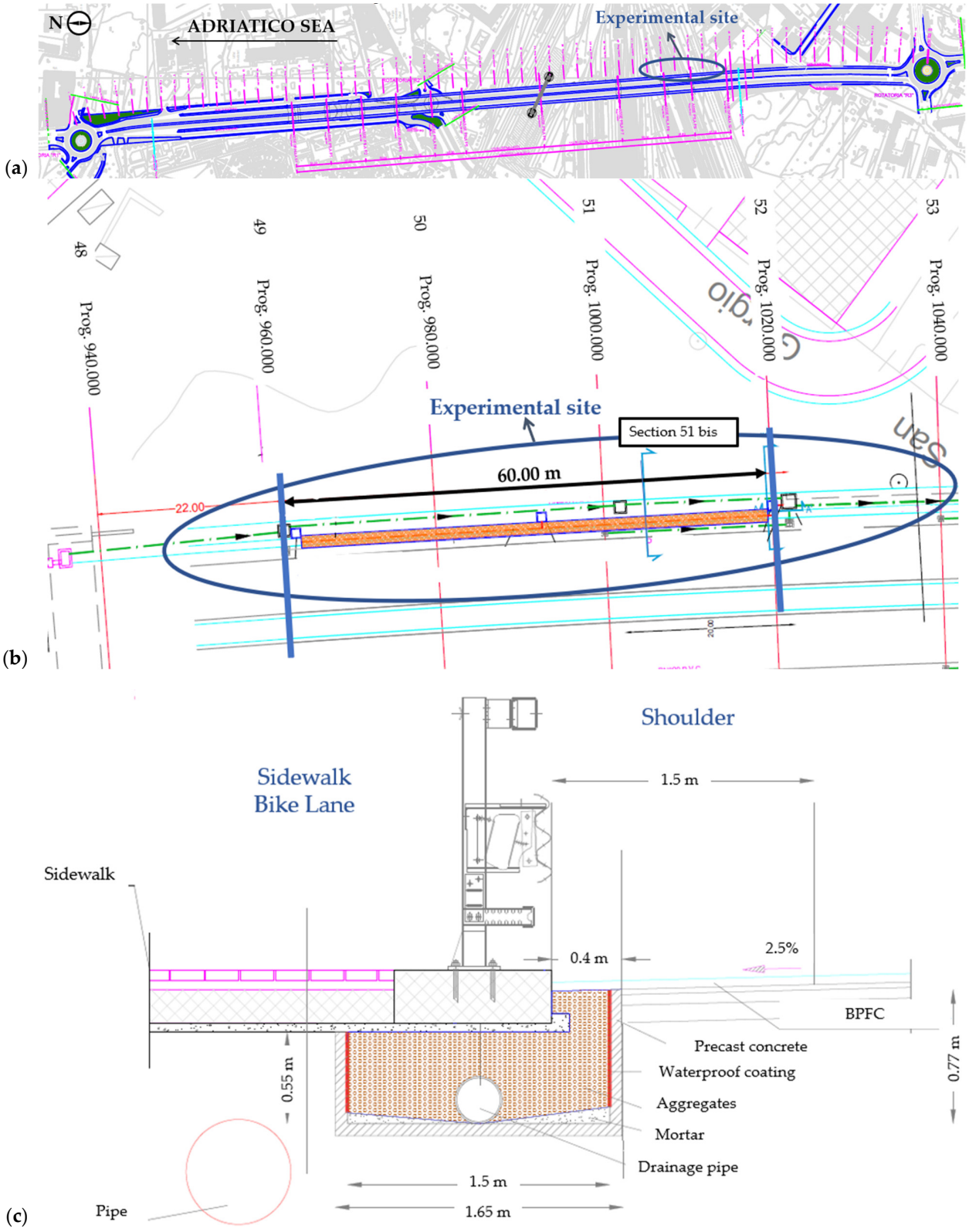

Figure 2. (**a**) Plan view of the bridge. (**b**) Plan view of the physical model included in the bridge. The infiltration trench is highlighted in orange. (**c**) Section view of the physical-model system excerpted and highlighted from the plan view.

Figure 2 shows the plan view of the bridge and, in detail, the section view through the physical model of the runoff treatment system. The BPFC area of the system is shown in

grey, while the infiltration trench is shown in orange, which runs parallel to the pipeline sewer (dashed green line with arrows).

During a storm event, rainfall is translated to runoff at the pavement surface, entraining previously dry PM deposition into the shallow overland pavement flow. This shallow flow infiltrates into the permeable pavement and is transported through the permeable pavement with a geodetic slope of 4.88%. The water is conveyed through the permeable pavement into the infiltration trench. The water passes through the trench with vertical filtration, and it is collected by the micro-slotted pipe. As a result, primary and secondary filtration unit operations in series are provided by the system. The filtered water can be collected through the inspection chambers for analysis. At the end of the physical model, the treatment water is discharged into the sewer system.

The methods used for this analysis are described as follows.

2.3. Methods

2.3.1. Methods for the Physical-Model Configuration

The definition of the BPFC+AGG system functionality requires several steps, which are outlined in Figure 3. Each of the methods of examination were needed to ensure the functionality of the system and the system response to rainfall, runoff, and PM loadings. The goal of the physical model that is presented herein is to provide a framework for the design and validation of the combined BPFC+AGG system.

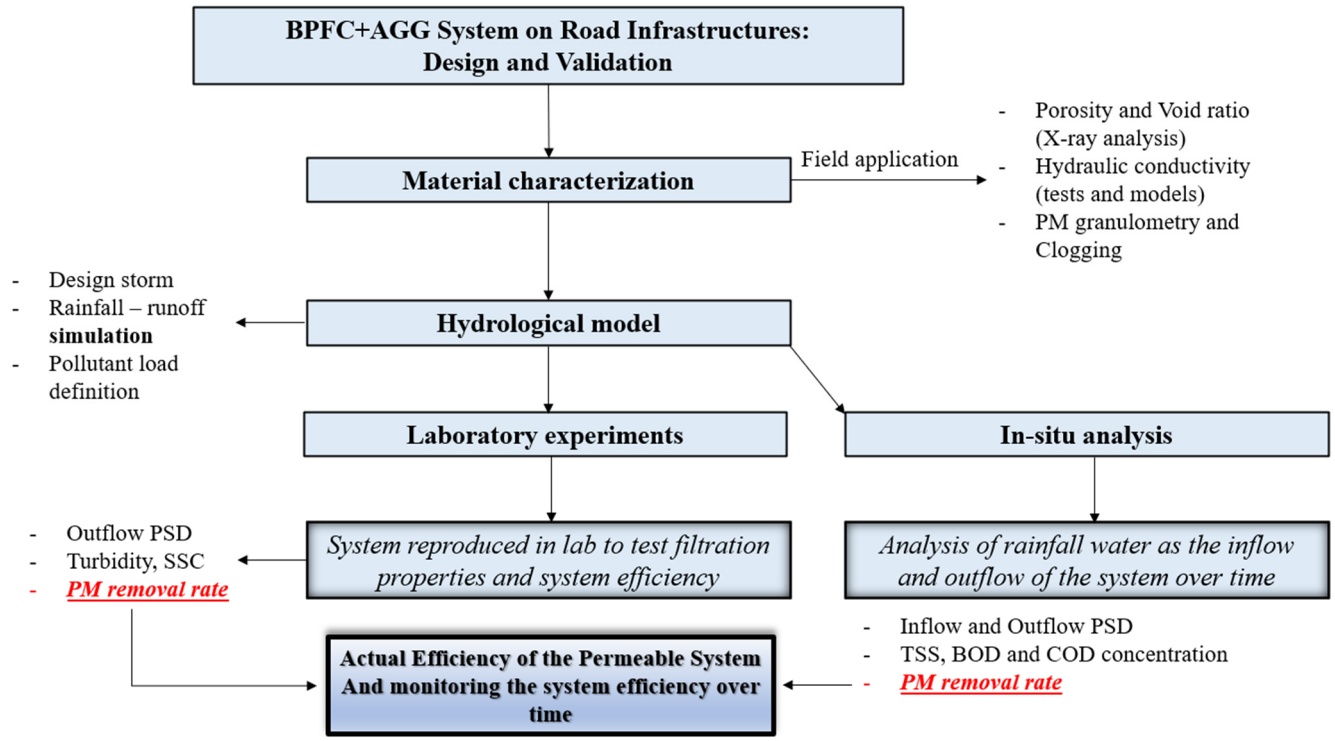

Figure 3. Methodological framework for the delineation of the filtration properties of the asphalt BPFC+AGG system. PSD: particle size distribution. SSC: suspended-sediment concentration (a gravimetric measure of all PM, not just the TSSs).

Figure 3 illustrates and extends the steps of the research outlined in the Introduction. Figure 3 presents a framework dedicated to characterizing the infrastructure materials and system in terms of their hydraulic conductivity and porosity. These examinations can be conducted by means of X-ray tomography and computational fluid dynamic (CFD) models [45]. The loadings to the BPFC+AGG system include the rainfall, runoff hydraulics, and PM entrained and transported in the runoff. The interaction between the permeable matrix of the system and the PM granulometry is needed to quantify the filter ripening

(clogging), which depends on the granulometry of the PM and the pore size distribution of the permeable matrix. Sampling and analysis of the runoff and PM across multiple influent hydrographs is required to characterize the PM concentration, the load, and the PSD of the influent PM. A model of the head loss, such as Ergun [54] or Kozeny-Carman [55], is needed to examine the permeable matrix of the filtration system. This analysis provides an index for the head-loss trends and the potential maintenance (cleaning) frequency for the accreted specific deposit within the permeable matrix over time. This evaluation also allows for the examination of the BPFC+AGG system with respect to the PM filtration to quantify the treatment of the runoff.

The second step involves the determination of the runoff flowrates and volume across hydrographs loading the permeable matrix, which strongly influences the BPFC+AGG system response. The hydrological investigation is required either utilizing a design storm/return period analysis and/or a longer-term continuous simulation [56–58]. The hydrologic analyses inform the hydraulic evaluation. Therefore, after the hydrologic analyses, the determination of the hydraulic conductivity of the permeable matrices is required, one in the laboratory and the other an in situ analysis.

In the laboratory, the representative loading conditions for the permeable matrices of the physical-model system were reproduced to accurately test and investigate the permeable-system filtration process. These conditions included the PM granulometry and PM indices, including the turbidity. The particle size distribution (PSD) and particle number density (PND), which is an index for turbidity, were required to quantify the performance of the physical-model system.

With respect to in situ monitoring, influent, primary effluent, and secondary effluent were collected and analyzed. These analyses, based on the PM and flows, quantified the system efficiency primarily for sequestering PM, while also allowing for the testing of the system with respect to the regulation of the constituents and indices thereof (metals, hydrocarbons, PM as total suspended solids (TSSs), and chemical oxygen demand (COD)). With this passive infrastructure system efficiency potentially reducing the concentration and loads to below regulatory levels, ancillary or centralized treatment for runoff may no longer be needed, resulting in a potentially significant decrease in the infrastructure and management/maintenance costs of more centralized or satellite systems.

2.3.2. Methods for PM Characterization

PM is a mobile substrate with a high surface area to which chemicals and pathogens partition to and from, and it is a substrate that impacts the treatment functionality and potentially the failure modes; therefore, the management of PM is a primary objective, whether for stormwater (wet-weather) or wastewater (dry-weather) flows. Therefore, detailed PM characterization is required to support the treatment functionality and sustainability. PM analysis is required to assess the modes of interaction with the permeable system, including the functionality and failure, and, therefore, the sustainable design of the permeable system.

The permeable-pavement filtering ability mainly depends on the relationship between the PM PSDs and the filter pore size distributions, including those of the permeable pavement. Considering the mean pore diameter of the pavement (d_m and the PM particle diameter (d_p), three primary classes of filtration mechanisms can be identified [59–61]:

- Surficial straining : $\frac{d_m}{d_p} < 10$
- Deep-bed filtration : $10 < \frac{d_m}{d_p} < 20$
- Physical–chemical : $\frac{d_m}{d_p} > 20$

When surficial straining occurs, a filter cake of strained solids, a "schmutzdecke", is formed above the permeable-pavement surface due to the progressive accumulation of PM. This surficial layer leads to the clogging of the permeable matrix, but the schmutzdecke can retain the finer PM fraction, providing additional PM separation yet leading to potential clogging unless there is a plan for maintenance. When this mechanism is dominant, the hydraulic conductivity of the permeable pavement can be readily restored through surficial cleaning techniques (e.g., washing–vacuum sweepers) [62]. When the main filtration mechanism is deep-bed filtration, interception and sedimentation occur. This leads to the potential failure of the system given that these deeper specific deposits are much more difficult to recover than surficial straining deposits. With respect to finer PM, the physical–chemical forces between the finer PM and permeable medium occur when the ratio $\frac{d_m}{d_p}$ is larger than 20. In this case, Brownian motion, sedimentation, interception, and adsorption dominate the removal mechanisms [60]. Therefore, the knowledge of the PM granulometry associated with granulometric parameters such as the number–volume mean size (l_{nv}) and particle number density (PND) is crucial for determining the PM load, the association of chemicals with the PM diameters, and the dominant separation mechanisms [63].

Despite some existing literature based on these types of studies [64–66], a deep and comparative analysis of PM samples on asphalt pavement under different boundary conditions is lacking. In this context, the study herein presented is focused on PM composition.

Particle Size Distribution (PSD) and Particle Number Distribution (PND) analyses. Dry-deposition PM samples were collected from March 2014 to January 2016, from 8 roadways in Bari and Taranto in Apulia, Italy, spanning a distance of 87 km for these locations, as in Figure 4. The sampling sites were selected in different areas and with different characteristics to obtain a large range of PM compositions to validate the models studied in this work. Despite the distance between the locations, the hydrological characteristics are comparable in terms of the annual rainfall volume: 536 mm and 575 mm in Bari and Taranto (https://protezionecivile.puglia.it/annali-idrologici-parte-i-dati-storici. Lastly accessed on the 18 December 2023). The site selection was conducted also considering the road pavement type (i.e., pervious, or impervious (collection samples 2 and 3 are proximate to the physical-model facility)). This choice was justified with the goal of examining the potential differences for the PSDs between asphalt permeable pavements and traditional asphalt pavements, and between permeable pavements with different service lives.

Table 1 reports the characteristics of the sampling scenarios, such as the previous dry days (PDDs), days from last cleaning (DLCs), and weather conditions during the sampling, as well as the land uses and types of pavement.

For each site, 2 samples were collected for a total of 16 dry-deposition collection events. Sampling was performed manually by using a stiff nylon brush and stainless-steel trowel. The PM recovered was composed of inert (inorganic) and volatile (organic) materials, including soils, trash, litter, and biogenic matter (Figure 5).

The granulometric analysis of the collected samples was performed according to ASTM D421 for the sample preparation, and according to ASTM D422 (ASTM 1993) for the mechanical-sieving method, to obtain the PSDs. For the method validation, each PM sample was checked to ensure that the mass balance error remained below 2% with respect to the original mass.

The PNDs were determined for the samples. The particle number (Ni) for each particle size increment was determined according to Equation (1) [67]:

$$N_i = \frac{m_{i,\,norm}}{\rho_{s,i} V_{s,i}} \quad (1)$$

where

- $\rho_{s,i}$ is the particle density for the i-th particle size, assumed to be equal to 2.65 g/cm^3 for all the particle sizes [68];

- $V_{s,i}$ is the particle volume of the i-th particle size. According to [69], a spherical shape of the particles was assumed. Thus, the volume of the sphere was calculated considering as a diameter the d_{median} (i.e., the median particle diameter (µm)): $V_{s,i} = \frac{\pi}{6} d_{median}{}^3$;
- $m_{i,norm}$ is the dry mass normalized to 1000 g of the i-th particle size, as in Equation (2):

$$m_{i,norm} = m_i \frac{1000}{M_{tot}} \quad (2)$$

It is possible to define another parameter related to the N_i: the number–volume mean size (l_{nv}), which is defined as the weighted average of the particle diameters based on both the number and volume of particles for a given size fraction. The l_{nv} for the overall particle gradation can be calculated according to Equation (3). In this equation, l_i is the representative particle diameter for the i-th particle size:

$$l_{nv} = \sqrt[3]{\frac{\sum N_i l_i^3}{\sum N_i}} \quad (3)$$

Figure 4. (**a**) Location of Apulia in Italy; (**b**) locations of Bari and Taranto in Apulia highlighted by red stars. All the main cities of the region are shown. BAT stands for the province made by Barletta-Andria-Trani; (**c**) sampling sites in Bari: 1. Via Napoli; 2. Via Sangiorgi; 3. Via Tatarella; 4. Via Cairoli; 5. Via Dante; (**d**) sampling sites in Taranto: 6. Viale Cannata; 7. Viale Magna Grecia; 8. Strada Statale 7.

Table 1. Detailed information of PM collected at sampling sites.

Specimen ID [a]	Sampling Date	Weather [b]	PDD [c]	DLC [d]	Pavement Type	Land Use	AADT [e]
BA_CAIROLI_1	05 Nov 15	clear	6	0	impervious	residential	6289
BA_CAIROLI_2	09 Jan 16	p. cloudy	2	3	impervious	residential	6289
BA_DANTE_1	05 Nov 15	clear	6	-	impervious	residential	17,444
BA_DANTE_2	09 Jan 16	p. cloudy	2	5	impervious	residential	17,444
BA_NAPOLI_1	20 Mar 14	clear	8	10	impervious	commercial	29,469
BA_NAPOLI_2	09 Jan 16	p. cloudy	2	17	impervious	commercial	29,469
BA_SANGIORGI_1	20 Mar 14	clear	8	-	permeable	commercial	44,955
BA_SANGIORGI_2	09 Jan 16	p. cloudy	2	-	permeable	commercial	44,955
BA_TATARELLA_1	20 mar 14	clear	8	-	permeable	commercial	29,744
BA_TATARELLA_2	09 Jan 16	p. cloudy	2	-	permeable	commercial	29,744
TA_CANNATA_1	23 Mar 14	p. cloudy	11	-	impervious	residential	16,086
TA_CANNATA_2	31 Dec 15	p. cloudy	34	-	impervious	residential	16,086
TA_MAGNAGRECIA_1	23 Mar 14	p. cloudy	11	11	impervious	residential	43,233
TA_MAGNAGRECIA_2	31 Dec 15	p. cloudy	34	19	impervious	residential	43,233
TA_SS7_23_1	23 Mar 14	p. cloudy	11	-	impervious	industrial	12,199
TA_SS7_31_2	31 Dec 15	p. cloudy	34	-	impervious	industrial	12,199

Note: Via Dante and Via Cairoli are one-way streets. All the others are two-way streets. [a] Specimen ID: city code_streets_sampling order (1 for first; 2 for second); i.e., BA stands for Bari and TA stands for Taranto. [b] Weather conditions at the time of collection: cloudy; partially cloudy (p. cloudy); clear. [c] Previous dry days (PDDs). [d] Days from last cleaning (DLCs). [e] Annual average daily traffic (vehicles/day).

Once these parameters were determined, the cumulative PM mass distribution and the PSD were modeled. A cumulative gamma distribution function was implemented, with the assumption of spherical particles. In this regard, the gamma distribution parameters were the scale and shape factors (θ and γ) and the particle diameter (d) (μm), according to [17].

The method of the minimization of the sum of squared errors (SSE) was used for the parameter estimation. The Kolmogorov–Smirnov test (K-S) was used to check whether the gamma distribution was suitable to represent the measured PSD data [70]. If the null hypothesis was retained (p-value > 0.05), then it could be concluded that the two samples of the measured and modeled data were drawn from the same population.

As for the cumulative PND, it is possible to use a model relying on a two-parameter power law model (PLM), as in Equation (4) [71]:

$$N_i = \alpha(l_{nv.i})^{-\beta} \quad (4)$$

where

- α is an empirical constant for a given particle gradation, which accounts for the variability in the PM;
- β is an empirical constant, which describes the slope of the PLM particle distribution. β can be related physically to filtration mechanisms.

These parameters were calculated through the least-squares method to characterize the granulometric mass and indices as a function of the PM size gradation [63].

Comparison between samples.

After the analysis of the PM, these results were correlated to the boundary conditions present at each site to examine how to transfer the results to other contexts. This goal was facilitated with K-S statistical analyses. The main analysis performed was as follows, comparing different samples:

1. A comparison between each pair of PM samples collected from the same site on two different dates to obtain the potential influence of the sampling time on the PM;
2. A comparison between samples collected from permeable-pavement-equipped sites (Via Sangiorgi and Via Tatarella) and samples collected from traditional pavement-equipped sites. Just one site was used as the benchmark for traditional pavements (i.e., Via Napoli, since it showed similar traffic and land-use conditions to the sites with permeable pavements). Hence, the comparisons were as follows: Via Tatarella—Via Napoli and Via Sangiorgi—Via Napoli;

3. A comparison among 5 combinations of PM samples from sites with different land uses and traffic characteristics, as listed below:
   - Via Dante (Bari) vs. Via Cairoli (Bari): same land use, different traffic volume;
   - Via Dante (Bari) vs. Viale Magna Grecia (Taranto): same land use, different traffic volume;
   - Via Dante (Bari) vs. Viale Cannata (Taranto): same land use and same traffic volume;
   - Via Napoli (Bari) vs. Viale Cannata (Taranto): different land use and different traffic volume.
   - Viale Cannata (Taranto) vs. SS7 (Taranto): different land use and similar traffic volume.

The results are shown and discussed in the following section.

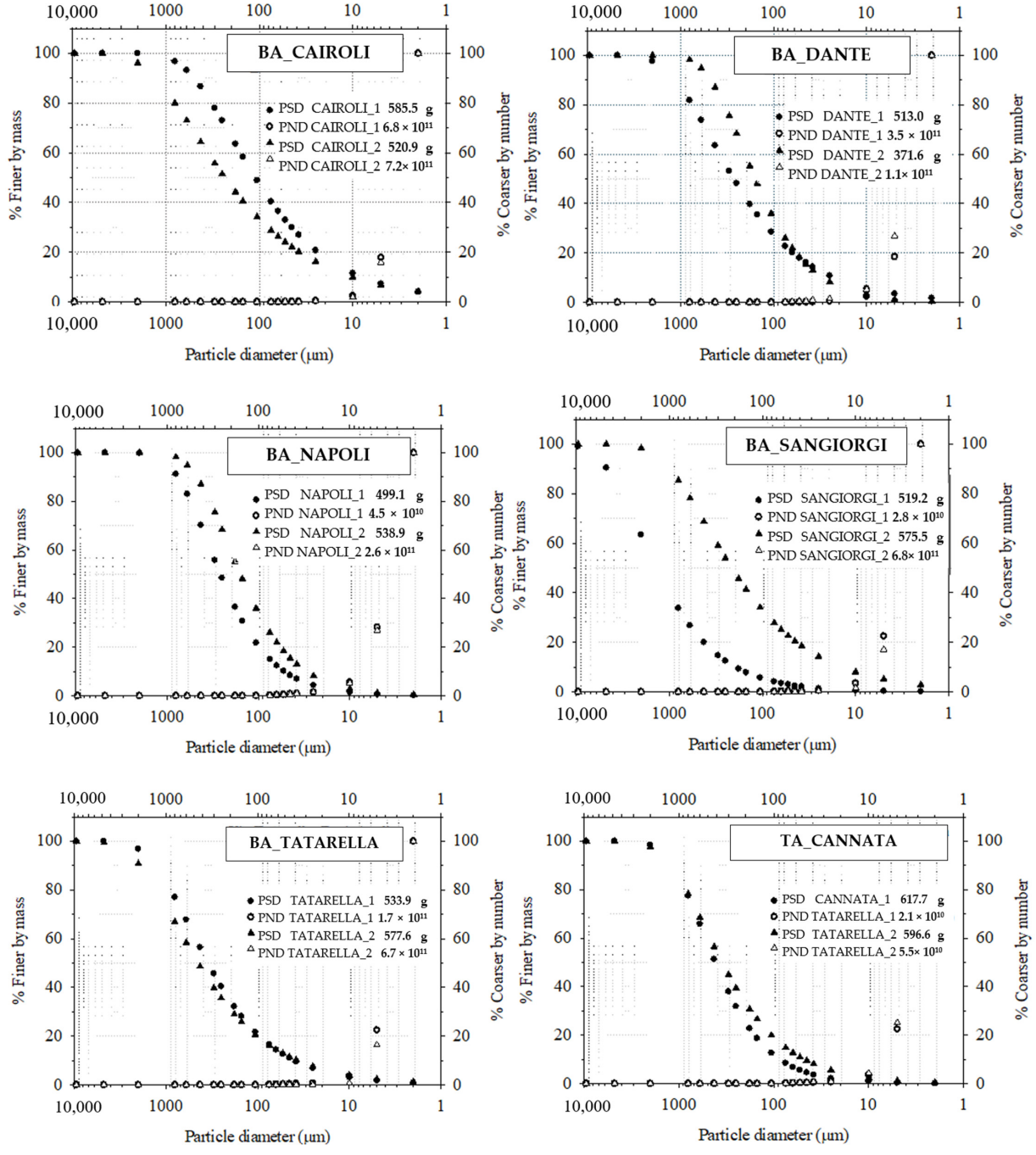

Figure 5. *Cont.*

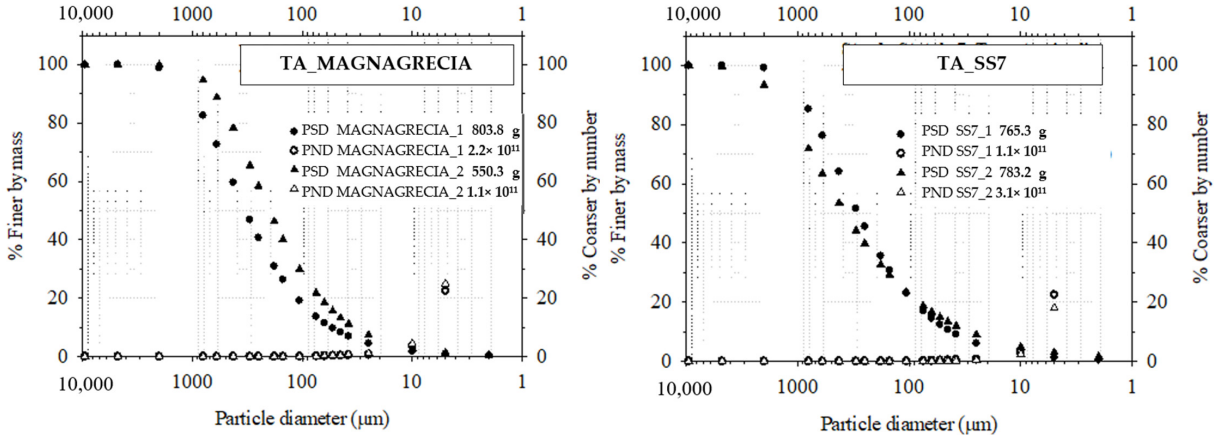

Figure 5. Particle size distribution (PSD) and particle number density (PND) for sediment from the 8 sites. Each graph contains the results from the two different sample collections.

3. Results and Discussion

3.1. PSD and PND Analysis Results

Starting from the PSDs of the 16 samples, the suitability of a simple two-parameter gamma distribution (Table 2) is shown. All 16 samples show comparable mass-based gradation (see Figure 5). The finer fraction of PM (< 75 µm) is included in the range of 4–40%, the extremes of which belong to the samples BA_SANGIORGI_1 and BA_CAIROLI_1. When comparing the two different samples at the same site, the difference in terms of the finer fraction (< 75 µm) between the two samples falls within the 10% range, except for BA_CAIROLI_1, and BA_SANGIORGI_1, which show extreme values.

Table 2. Summary of Kolmogorov–Smirnov statistics (k-s) for cumulative γ distribution fitted to dry-sediment particle size distributions. Summary of dry-deposition PM collected at roadways based on ASTM 1993 [17].

Specimen ID	Gamma Parameter		Test Statistics				Particle Diameter Indexes				C_u
	γ [(a)]	θ [(b)]	SSE [(c)]	K-S	*p*-Value	h-null [(d)]	d_{10} (µm)	d_{50} (µm)	d_{60} (µm)	d_{90} (µm)	
BA_CAIROLI_1	1.11	11.67	0.38	0.29	0.35	true	8	111	332	514	44.7
BA_CAIROLI_2	0.54	900.99	217.19	0.15	0.59	true	10	236	797	2000	79.5
BA_DANTE_1	0.71	637.98	136.78	0.15	0.96	true	23	268	748	2000	32.8
BA_DANTE_2	1.18	181.91	222.73	0.15	0.96	true	30	158	364	490	12.2
BA_NAPOLI_1	1.24	261.68	190.56	0.15	0.96	true	52	260	598	800	11.5
BA_NAPOLI_2	0.78	526.29	539.32	0.12	0.99	true	26	256	700	2000	26.9
BA_SANGIORGI_1	0.96	2084.51	64.82	0.2	0.78	true	195	1455	3074	9500	15.7
BA_SANGIORGI_2	0.64	612.51	283.81	0.15	0.96	true	15	216	697	1230	47.5
BA_TATARELLA_1	0.64	646.77	508.37	0.15	0.96	true	38	351	942	2000	24.8
BA_TATARELLA_2	0.7	1089.07	332.3	0.17	0.89	true	37	449	1339	1747	36.5
TA_CANNATA_1	1.29	421.97	110.71	0.15	0.96	true	87	413	891	2000	10.3
TA_CANNATA_2	1.1	448.33	156.11	0.15	0.96	true	63	359	861	2000	13.7
TA_MAGNAGRECIA_1	1.07	433.76	242.1	0.14	0.98	true	55	331	833	2000	15.3
TA_MAGNAGRECIA_2	1.08	258.06	278.98	0.15	0.96	true	34	201	475	641	14.1
TA_SS7_23_1	0.98	425.64	283.6	0.15	0.96	true	42	286	684	2000	16.3
TA_SS7_31_2	0.69	948.49	111.24	0.15	0.96	true	29	378	1069	2000	36.3

[(a)] γ is the shape factor of the gamma distribution function. [(b)] θ is the scale factor of the gamma distribution function. [(c)] The sum of squared errors (SSE). [(d)] Hypothesis—null: the samples are drawn from identical distributions with ($p > 0.05$), true or false.

The granulometric indexes are reported in Table 2 for each collected and analyzed sample. These indexes represent the particle diameters at which 10% (d_{10}), 50% (d_{50}), 60% (d_{60}), and 90% (d_{90}) of the particle gradation mass is finer. It is remarkable to note the results for the d_{50}: the mean is 358 µm (with a standard deviation of 306 µm), suggesting that all the d_{50} fell in the sand-size range. As already highlighted, the samples BA_CAIROLI_1 and

BA_SANGIORGI_1, which show extreme values, present, respectively, the smallest and largest d_{50}, corresponding to fine sand and very coarse sand. Excluding the extreme values (BA_SANGIORGI_1 and BA_CAIROLI_1) from the mean calculation of the d_{50} decreases the mean value of the d_{50}, which becomes 297 µm. This result provides a clear indication about the pore dimensions of the BPFC. In fact, if the intent is to have the occurrence of surficial straining, the ratio between the pavement pores (d_{m50}) and PM particle diameters (d_{p50}) must be lower than 10. Thus, the d_{m50} of the BPFC is approximately 3 mm.

Moreover, when comparing the obtained results to the existing literature, the reported results of this work are in line with the existing ones. Lin et al. [72] had similar results (mean d_{50} = 421 µm ± 219 µm) investigating the PM granulometry collected from three Portland-concrete-paved urban roads and one asphalt-paved urban road in the USA. Not similar but comparable results for the d_{50} (ranging between 100 µm to 200 µm) were also found by Zhao et al. [73], who analyzed the dry-road PM collected from various land types in the urban area of Beijing, China.

In Table 2, the uniformity coefficients, calculated as shown in Equation (5), are also expressed, highlighting the uniformity of the PM particles, since the coefficients range from 10.3 to 47.5:

$$C_u = \frac{d_{60}}{d_{10}} \quad (5)$$

With respect to the particle number density, the PNDs were plotted as a percentage of the coarser particles, considering their quantity by number and not by mass (see Figure 5). The number of particles increased with the decrease in the diameter for each sample. This trend is in contrast with the one shown by the PSD curve (particle mass decrease with size).

This inverse relationship is shown by all the analyzed PM samples. Trying to investigate the PNDs with the PLM, the parameters l_{nv} and N_i were plotted together by a log–log relationship, to compare the measured data against the modeled results (Figure 6). The results illustrate a good fit for each site, as also highlighted in Table 3, and all the coefficients of determination exceed 0.92. However, the absolute values of the α coefficient in Equation (4) are variable (ranging from 5×10^{12} to 2×10^{14}), indicating that the particle number is subjected to huge variation from site to site, driven by the finer silt- and clay-size fractions. The β exponent in Equation (4) ranged from 2.27 to 3.30. The results indicate that the larger the value of β, the larger the contribution of the smaller particles, in line with previous literature [63].

Table 3. PLM parameters of particle number density (PND) for each site and coefficients of determination (R^2).

Specimen ID	$N_i = \alpha\ (l_{nv,i})^{-\beta}$ [a]		
	α	**β**	**R^2**
BA_CAIROLI_1	2×10^{14}	3.30	0.98
BA_CAIROLI_2	2×10^{13}	2.92	0.99
BA_DANTE_1	4×10^{13}	3.08	0.96
BA_DANTE_2	1×10^{14}	3.26	0.97
BA_NAPOLI_1	2×10^{13}	2.90	0.96
BA_NAPOLI_2	3×10^{13}	3.05	0.95
BA_SANGIORGI_1	3×10^{11}	2.27	0.97
BA_SANGIORGI_2	3×10^{13}	2.97	0.92
BA_TATARELLA_1	5×10^{12}	2.68	0.99
BA_TATARELLA_2	6×10^{12}	2.70	0.98
TA_CANNATA_1	8×10^{12}	2.83	0.93
TA_CANNATA_2	6×10^{12}	2.74	0.96
TA_MAGNAGRECIA_1	5×10^{12}	2.71	0.97
TA_MAGNAGRECIA_2	2×10^{13}	2.95	0.98
TA_SS7_23_1	6×10^{12}	2.72	0.98
TA_SS7_31_2	2×10^{13}	2.87	0.97

[a] The basic form of the two-parameter power law function adopted. *Ni* is the particle count for each particle size increment. The number–volume mean size ($l_{nv,i}$) is the weighted average of the particle diameter. The method of least squares was used for the parameter estimation.

The sample BA_CAIROLI_1, as already found for the PSD, shows a larger contribution of finer particles (<75 µm) than the other sample particles. This trend is probably due to the mechanical sweeping performed by road agents less than 24 h before the sampling (see Table 1), which recovered coarse PM. A different behavior was shown by the sample collected on the porous asphalt pavement BA_SANGIORGI_1, which has a reduced contribution of smaller particles compared to the other samples, including the sample collected on the same street around one and a half years later.

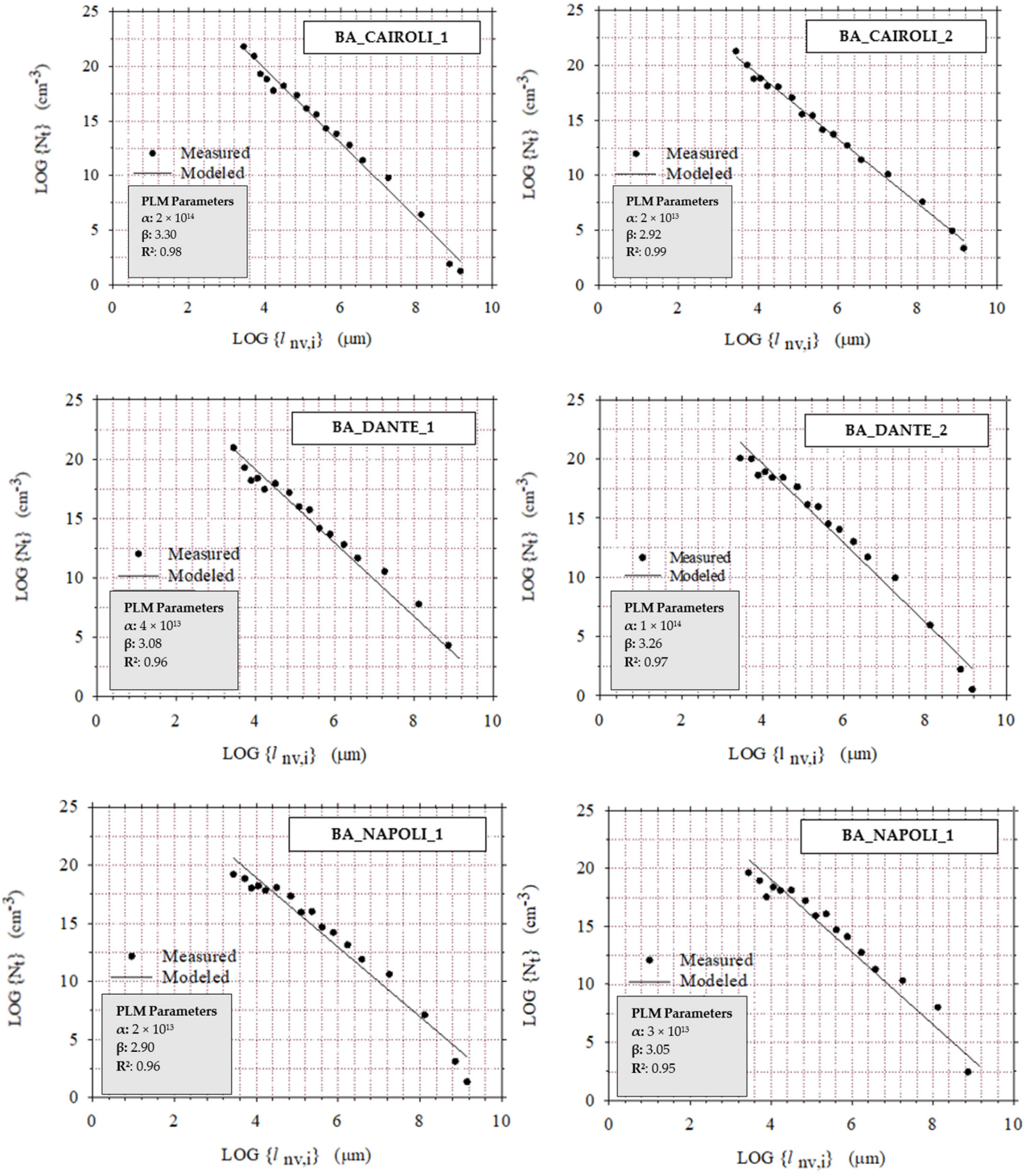

Figure 6. *Cont.*

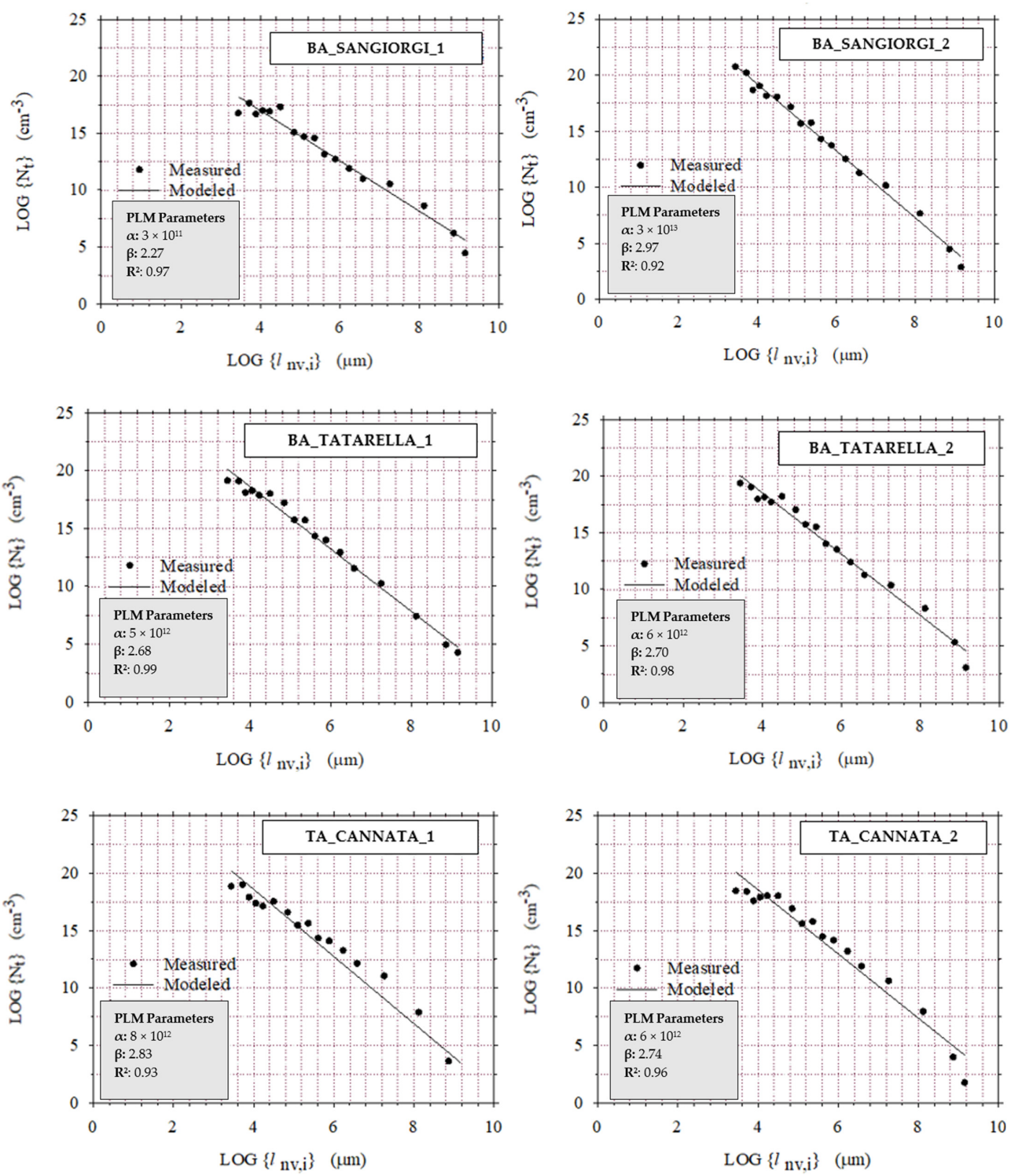

Figure 6. *Cont.*

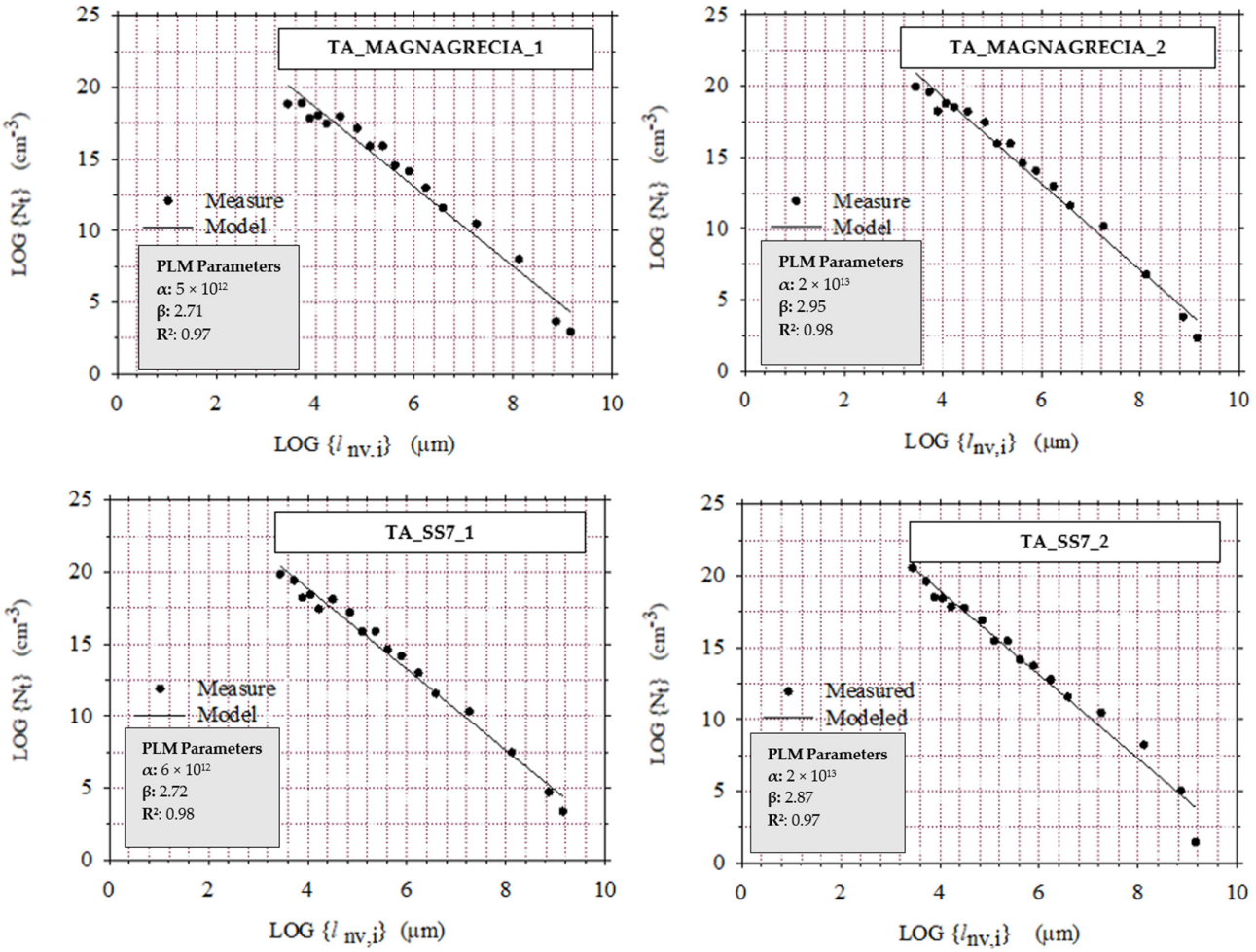

Figure 6. Fit of data by the power law function from the 8 sites for each of the two collections.

This is one of the most tangible effects of the clogging over time. Even if, in this analysis, just two collections per site were made at different times, the differences between the two collections start providing different results due to the insurgence of the clogging effect. The clogging occludes the porous pores that trap the particles and reduces the particle gradations passing. In these conditions, the PSD and PND tend to vary.

Despite these first considerations about clogging, more detailed results and analysis about the clogging and its mechanism and interaction with pores will be dealt with in future works within the proposed framework, accounting for different time horizons to deeply investigate the clogging effects.

3.2. Results of Comparison between Samples

The comparison between the different samples was investigated by K-S analysis, which assessed whether two samples, collected from the same site on different dates, were represented by the same population. As already highlighted for the other results, the only samples that were statistically different were those collected in Via Sangiorgi (Bari), which showed a *p*-value equal to 0.008.

The exceptionality of the samples from Via Sangiorgi has been confirmed, also examining other comparative analyses. BA_SANGIORGI_1 always has a different behavior with respect to the other samples. The permeable pavement in Via Sangiorgi was laid during 2013, and the first sampling (20 March 2014) was performed about 6 months later, while the second sampling was performed about 2 years later (9 January 2016). During this lifetime period of the permeable pavement, regular cleaning procedures (not specific for permeable pavements) were performed. Therefore, in the period between the two samplings, the

pavement seems to have clogged up. In the first sampling, the pores were still clean, and the finer particles could drop into the interval matrix, so that the mechanical sweeping that operated during the sampling was unable to collect these finer particles. In the second sampling, the pavement was more clogged, and the finer particles could be collected on the pavement surface, as the pavement was no longer able to filter them. This justifies the difference in the sample particle gradations. This result can be confirmed by comparing the two PSDs of Via Sangiorgi with those collected from the other commercial streets with comparable traffic volumes (Table 4). With the intent of understanding whether this behavior is common to permeable pavements, the PSDs of Via Tatarella and Via Sangiorgi were compared to the PSD of Via Napoli (9 January 2016) by means of the K-S results (Table 4), since Via Tatarella is also paved with a permeable pavement and presents the same boundary conditions as those of Via Sangiorgi. The Via Tatarella pavement was installed about 10 years earlier than the one in Via Sangiorgi and has never been cleaned with a specific cleaning procedure. However, the results of the tests (Table 4) highlight that the two permeable pavements behave differently when compared to the impervious pavement at the beginning of its service life. Both the samples collected in Via Tatarella and the second sample collected in Via Sangiorgi, after years of no applications of specific cleaning procedures, have similar compositions to the reference samples collected from the impervious pavement.

The statistical K-S analysis was also performed for all the other PSD results to determine whether the samples, with different land uses and traffic volumes, are represented by the same population. Table 4 shows the comparison between each pair of sites with different environmental and traffic characteristics, regardless of the cities. The results show no statistical differences in the samples for each combination. The samples belong to the same population in terms of the PSDs. PSD similarities with different sites with comparable boundary conditions were also found in the literature for different types of permeable pavements, such as CPP [74]. Moreover, always considering pervious concrete materials, it seems that the PSD is not much influenced by other variables [26]. With respect to CPP, it was found that cleaning procedures enhance the efficiency of the system, providing a better PM removal performance [23]; thus, the two sites of Via Tatarella and Via Sangiorgi could have shown different PSD results after specific cleaning procedures. Considering the asphalt permeable pavement and the contaminant removal, it seems that there is a significant difference in the contaminants, more than for the PSD, between pervious and impervious asphalt [26]. However, this aspect will be further investigated in the development of this research, as stated when the general set-up was presented.

Table 4. Summary of Kolmogorov–Smirnov statistics (K-S) for cumulative distribution PSDs of PM samples for the three proposed comparisons in Section 2.3.2.

	Specimen IDs		**Test Statistics**		
	Sample 1	**Sample 2**	**K-S**	***p*-Value**	**h-Null**
First comparison: differences between the two collections at the same site	BA_CAIROLI_1	BA_CAIROLI_2	0.20	0.77	true
	BA_DANTE_1	BA_DANTE_2	0.15	0.97	true
	BA_NAPOLI_1	BA_NAPOLI_2	0.20	0.77	true
	BA_SANGIORGI_1	BA_SANGIORGI_2	0.50	8.20×10^{-3}	false
	BA_TATARELLA_1	BA_TATARELLA_2	0.10	0.99	true
	TA_CANNATA_1	TA_CANNATA_2	0.15	0.97	true
	TA_MAGNAGRECIA_1	TA_MAGNAGRECIA_2	0.15	0.97	true
	TA_SS7_1	TA_SS7_2	0.10	0.99	true
Second comparison: Permeable—impervious pavement	BA_NAPOLI_1	BA_NAPOLI_2	0.20	0.77	true
	BA_TATARELLA_2	BA_NAPOLI_2	0.16	0.97	true
	BA_TATARELLA_1	BA_NAPOLI_2	0.16	0.97	true
	BA_SANGIORGI_2	BA_NAPOLI_2	0.16	0.97	true
	BA_SANGIORGI_1	BA_NAPOLI_2	0.47	0.03	false

Table 4. *Cont.*

	Specimen IDs		Test Statistics		
	Sample 1	**Sample 2**	**K-S**	***p*-Value**	**h-Null**
Third comparison: differences between sites with different land uses and traffic	BA_DANTE_1	BA_CAIROLI_1	0.26	0.53	true
	BA_DANTE_1	BA_CAIROLI_2	0.16	0.97	true
	BA_DANTE_2	BA_CAIROLI_1	0.26	0.53	true
	BA_DANTE_2	BA_CAIROLI_2	0.16	0.97	true
	BA_DANTE_1	TA_MAGNAGRECIA_1	0.26	0.53	true
	BA_DANTE_1	TA_MAGNAGRECIA_2	0.11	1.00	true
	BA_DANTE_2	TA_MAGNAGRECIA_1	0.21	0.79	true
	BA_DANTE_2	TA_MAGNAGRECIA_2	0.11	1.00	true
	BA_DANTE_1	TA_CANNATA_1	0.32	0.30	true
	BA_DANTE_1	TA_CANNATA_2	0.26	0.53	true
	BA_DANTE_2	TA_CANNATA_1	0.32	0.30	true
	BA_DANTE_2	TA_CANNATA_2	0.26	0.52	true
	BA_NAPOLI_1	TA_CANNATA_1	0.21	0.79	true
	BA_NAPOLI_1	TA_CANNATA_2	0.11	1.00	true
	BA_NAPOLI_2	TA_CANNATA_1	0.32	0.30	true
	BA_NAPOLI_2	TA_CANNATA_2	0.26	0.53	true
	TA_CANNATA_1	TA_SS7_1	0.26	0.53	true
	TA_CANNATA_1	TA_SS7_2	0.32	0.30	true
	TA_CANNATA_2	TA_SS7_1	0.16	0.97	true
	TA_CANNATA_2	TA_SS7_2	0.21	0.79	true

4. Conclusions

Given the increase in infrastructure and buildings, there is a need to include pavement system designs and implementation based on environmental and human health. This research is aligned with this need. In this work, the authors present a full-scale physical model designed for a permeable system constructed of a bituminous-pavement open-graded friction course (BPFC) combined with an infiltration trench made with natural aggregates (AGGs). The BPFC-AGG is indicated for cases in which the high mechanical resistance required cannot be handled by a full-depth PAS.

The proposed pavement system is already installed at the Adriatico Bridge, in Bari (Italy), as a full-scale physical model. This physical model was used as a reference for all the laboratory tests (run both at the Polytechnic University of Bari and at the University of Florida). Some results related to the first steps of the proposed physical-model work have been already investigated.

As the first step of the research, the characterization of typical PM accreted on public roads is presented, in terms of the PND and PSD. The analysis showed that the mean pore size of the BPFC might be at least 3 mm, inducing only surficial straining in the case of clogging occurrence. This result came from the analysis of 16 samples collected at eight different sites with different land uses, traffic, and pavements from different cities, to extend the outputs to different configurations. Regarding the PSDs and PNDs of the samples, the results indicated that all the collected PM showed similar distributions, except for two samples, because of their site characteristics. The PSD of the PM showed a largely sand-size gravimetric distribution. The PND was modeled by the Power Law Model (PLM). The model fit the measured granulometry results (coefficients of determination are always greater than 0.92). Comparing all the sample results by means of K-S statistics, the results indicate that the different boundary conditions did not significantly influence the PM size distribution for all but two locations. Lastly, the permeable pavements without the use of a periodic common cleaning program (with equipment intended for permeable pavements) is subject to eventual clogging, as the permeable matrix is a filter and temporary repository for PM and runoff chemicals, whether adsorbed by the PM or the high surface area of the pore space.

As previously stated, this is just the first result of wider research, the steps of which will be further investigated and detailed. For this reason, in this manuscript, the effects of clogging on the PSD, PND, and pavement performance over time were neglected, since these topics are part of the future development of this research.

Author Contributions: Conceptualization, V.R., V.F. and J.J.S.; methodology, V.R. and J.J.S.; validation, V.R. and J.J.S.; formal analysis, V.F. and S.C.; investigation, V.F. and S.C.; resources, V.R. and J.J.S.; data curation, S.C., V.F. and P.I.; writing—original draft preparation, S.C and V.F.; writing—review and editing, S.C., P.I. and V.R.; visualization, S.C.; supervision, V.R. and J.J.S.; project administration, V.R. and J.J.S. All authors have read and agreed to the published version of the manuscript.

Funding: This research received no external funding.

Data Availability Statement: All the data will be shared upon reasonable request.

Conflicts of Interest: The authors declare no conflicts of interest.

References

1. United Nations Department of Economic and Social Affairs. *World Urbanization Prospects, The 2018 Revision*; United Nations: New York, NY, USA, 2019.
2. Scalenghe, R.; Marsan, F.A. The anthropogenic sealing of soils in urban areas. *Landsc. Urban Plan.* **2009**, *90*, 1–10. [CrossRef]
3. National Research Council; Committee on Climate Change; US Transportation; Transportation Research Board; Division on Earth, & Life Studies. *Potential Impacts of Climate Change on US Transportation: Special Report 290 (Volume 290)*; Transportation Research Board: Washington, DC, USA, 2008.
4. European Commision. Eurostat. October 2022. Available online: https://ec.europa.eu/eurostat/statistics-explained/index.php?title=Urban-rural_Europe_-_introduction#Population_density (accessed on 10 November 2023).
5. Institute for European Environmental Policy. Environmental Threats to Rural Areas. March 2022. Available online: https://ieep.eu/news/environmental-threats-to-rural-areas/#:~:text=Soil%20and%20water%20health%20and,the%20regulation%20of%20freshwater%20quality (accessed on 10 November 2023).
6. Jandacka, D.; Decky, M.; Hodasova, K.; Pisca, P.; Briliak, D. Influence of the urban intersection reconstruction on the reduction of road traffic noise pollution. *Appl. Sci.* **2022**, *12*, 8878. [CrossRef]
7. Rossi, M.L.; Kremer, P.; Cravotta, C.A.; Scheirer, K.E.; Goldsmith, S.T. Long-term impacts of impervious surface cover change and roadway deicing agent application on chloride concentrations in exurban and suburban watersheds. *Sci. Total Environ.* **2022**, *851*, 157933. [CrossRef]
8. Chithra, S.V.; Nair, M.H.; Amarnath, A.; Anjana, N.S. Impacts of impervious surfaces on the environment. *Int. J. Eng. Sci. Invent.* **2015**, *4*, 27–31.
9. Yao, L.; Wei, W.; Chen, L. How does imperviousness impact the urban rainfall-runoff process under various storm cases? *Ecol. Indic.* **2016**, *60*, 893–905. [CrossRef]
10. Pappas, E.A.; Smith, D.R.; Huang, C.; Shuster, W.D.; Bonta, J.V. Impervious surface impacts to runoff and sediment discharge under laboratory rainfall simulation. *Catena* **2008**, *72*, 146–152. [CrossRef]
11. Kim, H.; Jeong, H.; Jeon, J.; Bae, S. The impact of impervious surface on water quality and its threshold in Korea. *Water* **2016**, *8*, 111. [CrossRef]
12. Xu, H. Analysis of impervious surface and its impact on urban heat environment using the normalized difference impervious surface index (NDISI). *Photogramm. Eng. Remote Sens.* **2010**, *76*, 557–565. [CrossRef]
13. Ranieri, V.; Coropulis, S.; Berloco, N.; Fedele, V.; Intini, P.; Laricchia, C.; Colonna, P. The effect of different road pavement typologies on urban heat island: A case study. *Sustain. Resilient Infrastruct.* **2022**, *7*, 803–822. [CrossRef]
14. Loganathan, P.; Vigneswaran, S.; Kandasamy, J. Road-deposited sediment pollutants: A critical review of their characteristics, source apportionment, and management. *Crit. Rev. Environ. Sci. Technol.* **2013**, *43*, 1315–1348. [CrossRef]
15. Bian, B.; Zhu, W. Particle size distribution and pollutants in road-deposited sediments in different areas of Zhenjiang, China. *Environ. Geochem. Health* **2009**, *31*, 511–520. [CrossRef]
16. Herngren, L.; Goonetilleke, A.; Ayoko, G.A. Analysis of heavy metals in road-deposited sediments. *Anal. Chim. Acta* **2006**, *571*, 270–278. [CrossRef] [PubMed]
17. Sansalone, J.; Ying, G. Partitioning and granulometric distribution of metal leachate from urban traffic dry deposition particulate matter subject to acidic rainfall and runoff retention. *Water Res.* **2008**, *42*, 4146–4162. [CrossRef] [PubMed]
18. Duong, T.T.; Lee, B.K. Determining contamination level of heavy metals in road dust from busy traffic areas with different characteristics. *J. Environ. Manag.* **2011**, *92*, 554–562. [CrossRef] [PubMed]
19. U.S. Environmental Protection Agency. *EPA's Report on the Environment*; U.S. Environmental Protection Agency: Washington, DC, USA, 2003.
20. Xie, N.; Akin, M.; Shi, X. Permeable concrete pavements: A review of environmental benefits and durability. *J. Clean. Prod.* **2019**, *210*, 1605–1621. [CrossRef]
21. Drake, J.; Bradford, A.; Van Seters, T. Stormwater quality of spring–summer-fall effluent from three partial-infiltration permeable pavement systems and conventional asphalt pavement. *J. Environ. Manag.* **2014**, *139*, 69–79. [CrossRef]
22. Zachary Bean, E.; Frederick Hunt, W.; Alan Bidelspach, D. Evaluation of four permeable pavement sites in eastern North Carolina for runoff reduction and water quality impacts. *J. Irrig. Drain. Eng.* **2007**, *133*, 583–592. [CrossRef]

23. Sansalone, J.; Kuang, X.; Ranieri, V. Permeable pavement as a hydraulic and filtration interface for urban drainage. *J. Irrig. Drain. Eng.* **2008**, *134*, 666–674. [CrossRef]
24. Sansalone, J.; Raje, S.; Kertesz, R.; Maccarone, K.; Seltzer, K.; Siminari, M.; Simms, P.; Wood, B. Retrofitting impervious urban infrastructure with green technology for rainfall-runoff restoration, indirect reuse and pollution load reduction. *Environ. Pollut.* **2013**, *183*, 204–212. [CrossRef]
25. Sansalone, J.; Kuang, X.; Ying, G.; Ranieri, V. Filtration and clogging of permeable pavement loaded by urban drainage. *Water Res.* **2012**, *46*, 6763–6774. [CrossRef]
26. Kayhanian, M.; Li, H.; Harvey, J.T.; Liang, X. Application of permeable pavements in highways for stormwater runoff management and pollution prevention: California research experiences. *Int. J. Transp. Sci. Technol.* **2019**, *8*, 358–372. [CrossRef]
27. Zhu, X.; Ye, F.; Cai, Y.; Birgisson, B.; Lee, K. Self-healing properties of ferrite-filled open-graded friction course (OGFC) asphalt mixture after moisture damage. *J. Clean. Prod.* **2019**, *232*, 518–530. [CrossRef]
28. Huang, X.; Song, J. Urban moisture and dry islands: Spatiotemporal variation patterns and mechanisms of urban air humidity changes across the globe. *Environ. Res. Lett.* **2023**, *18*, 103003. [CrossRef]
29. Lu, D.; Fu, C.; Jiang, X.; Chen, Z.; Qu, F.; Huo, Y.; Leng, Z.; Zhong, J. Sustainable microwave-heating healing asphalt concrete incorporating functional aggregates and waste ferrite. *Transp. Res. Part D Transp. Environ.* **2024**, *129*, 104117. [CrossRef]
30. Lu, D.; Jiang, X.; Leng, Z.; Zhang, S.; Wang, D.; Zhong, J. Dual responsive microwave heating-healing system in asphalt concrete incorporating coal gangue and functional aggregate. *J. Clean. Prod.* **2023**, *422*, 138648. [CrossRef]
31. Lu, D.; Jiang, X.; Leng, Z. Sustainable microwave-heating healing asphalt concrete fabricated with waste microwave-sensitive fillers. *J. Clean. Prod.* **2024**, *434*, 140343. [CrossRef]
32. Ranieri, V.; Colonna, P.; Sansalone, J.J.; Sciddurlo, A. Measurement of hydraulic conductivity in porous mixes. *Transp. Res. Rec.* **2012**, *2295*, 1–10. [CrossRef]
33. Ranieri, V. Drainage Issues Related to Porous Pavements. In *Atti del III SIIV International Congress*; SIIV: Bari, Italy, 2005; Volume 22, p. 24.
34. Legret, M.; Colandini, V. Effects of a porous pavement with reservoir structure on runoff water: Water quality and fate of heavy metals. *Water Sci. Technol.* **1999**, *39*, 111–117. [CrossRef]
35. Fach, S.; Dierkes, C. On-site infiltration of road runoff using pervious pavements with subjacent infiltration trenches as source control strategy. *Water Sci. Technol.* **2011**, *64*, 1388–1397. [CrossRef]
36. Myers, B.; Beecham, S.; van Leeuwen, J.A. Water quality with storage in permeable pavement basecourse. In *Proceedings of the Institution of Civil Engineers-Water Management*; Thomas Telford Ltd.: London, UK, 2011; Volume 164, pp. 361–372.
37. Li, H.; Li, Z.; Zhang, X.; Li, Z.; Liu, D.; Li, T.; Zhang, Z. The effect of different surface materials on runoff quality in permeable pavement systems. *Environ. Sci. Pollut. Res.* **2017**, *24*, 21103–21110. [CrossRef]
38. Zhang, K.; Yong, F.; McCarthy, D.T.; Deletic, A. Predicting long term removal of heavy metals from porous pavements for stormwater treatment. *Water Res.* **2018**, *142*, 236–245. [CrossRef] [PubMed]
39. Hammes, G.; Thives, L.P. Porous Asphalt Mixture with Improved Fatigue Resistance and Stormwater Pollutant Reduction in Urban Road Pavement. *Water* **2023**, *15*, 2962. [CrossRef]
40. Pezzaniti, D.; Beecham, S.; Kandasamy, J. Influence of clogging on the effective life of permeable pavements. In *Proceedings of the Institution of Civil Engineers-Water Management*; Thomas Telford Ltd.: London, UK, 2009; Volume 162, pp. 211–220.
41. Suarman, M.; Argue, J.R.; Pezzaniti, D. "Lifespan" of Permeable/Porous Paving Systems in" Source Control" Technology: First Results. *Urban Water Resour. Cent. Adel.* **1999**, *32*, 23–33, Internal report.
42. Boogaard, F.; Lucke, T.; Beecham, S. Effect of age of permeable pavements on their infiltration function. *CLEAN–Soil Air Water* **2014**, *42*, 146–152. [CrossRef]
43. Antunes, L.N.; Ghisi, E.; Thives, L.P. Permeable pavements life cycle assessment: A literature review. *Water* **2018**, *10*, 1575. [CrossRef]
44. Winston, R.J.; Al-Rubaei, A.M.; Blecken, G.T.; Viklander, M.; Hunt, W.F. Maintenance measures for preservation and recovery of permeable pavement surface infiltration rate–The effects of street sweeping, vacuum cleaning, high pressure washing, and milling. *J. Environ. Manag.* **2016**, *169*, 132–144. [CrossRef]
45. Fedele, V.; Berloco, N.; Colonna, P.; Hertrich, A.; Intini, P.; Ranieri, V.; Sansalone, J.J. Computational fluid dynamics as a tool to estimate hydraulic conductivity of permeable asphalts. *Transp. Res. Rec.* **2020**, *2674*, 370–383. [CrossRef]
46. Ranieri, V.; Berloco, N.; Colonna, P.; Fedele, V.; Sansalone, J.J. Granulometry of Particulate Matter Recovered from Roadway Systems in Apulia. In Proceedings of the Transportation Research Board 96th Annual Meeting Conference Abstract Proceedings—TRID No. 17-05066, Washington, DC, USA, 8–12 January 2017.
47. Harvey, J.; Shan, S.; Li, H.; Jones, D.J.; Wu, R. Fully permeable pavement for stormwater management: Progress and obstacles to implementation in California. *Airfield Highw. Pavements* **2017**, *2017*, 125–136.
48. de Graaf-van Dinther, R.; Leskens, A.; Veldkamp, T.; Kluck, J.; Boogaard, F. From Pilot Projects to Transformative Infrastructures, Exploring Market Receptivity for Permeable Pavement in The Netherlands. *Sustainability* **2021**, *13*, 4925. [CrossRef]
49. Ranieri, V. Runoff control in porous pavements. *Transp. Res. Rec. J. Transp. Res. Board* **2002**, *1789*, 46–55. [CrossRef]
50. Sambito, M.; Severino, A.; Freni, G.; Neduzha, L. A systematic review of the hydrological, environmental and durability performance of permeable pavement systems. *Sustainability* **2021**, *13*, 4509. [CrossRef]
51. Mullaney, J.; Lucke, T. Practical review of pervious pavement designs. *CLEAN–Soil Air Water* **2014**, *42*, 111–124. [CrossRef]

52. Mullaney, J.; Lucke, T. Permeable paving systems: Is there a potential use to promote street tree health, minimise pavement damage and reduce stormwater flows. In Proceedings of the 2013 Stormwater Industry Association Queensland State Conference, Townsville, Australia, 13–16 August 2013; Stormwater Industry Association: Queensland, Australia, 2013.
53. Fwa, T.F.; Lim, E.; Tan, K.H. Comparison of permeability and clogging characteristics of porous asphalt and pervious concrete pavement materials. *Transp. Res. Rec.* **2015**, *2511*, 72–80. [CrossRef]
54. Ergun, S. Fluid flow through packed columns. *Chem. Eng. Prog.* **1952**, *48*, 89.
55. Kozeny, J. Ueber kapillare leitung des wassers im boden. *Sitzungsberichte Akad. Wiss. Wien* **1927**, *136*, 271.
56. Papalexiou, S.M.; Koutsoyiannis, D. Battle of extreme value distributions: A global survey on extreme daily rainfall. *Water Resour. Res.* **2013**, *49*, 187–201. [CrossRef]
57. Shuster, W.D.; Bonta, J.; Thurston, H.; Warnemuende, E.; Smith, D.R. Impacts of impervious surface on watershed hydrology: A review. *Urban Water J.* **2005**, *2*, 263–275. [CrossRef]
58. Scholz, M.; Grabowiecki, P. Review of permeable pavement systems. *Build. Environ.* **2007**, *42*, 3830–3836. [CrossRef]
59. McDowell-Boyer, L.M.; Hunt, J.R.; Sitar, N. Particle transport through porous media. *Water Resour. Res.* **1986**, *22*, 1901–1921. [CrossRef]
60. Teng, Z.; Sansalone, J. In situ partial exfiltration of rainfall runoff. II: Particle separation. *J. Environ. Eng.* **2004**, *130*, 1008–1020. [CrossRef]
61. Marchioni, M.; Fedele, R.; Raimondi, A.; Sansalone, J.; Becciu, G. Permeable asphalt hydraulic conductivity and particulate matter separation with XRT. *Water Resour. Manag.* **2022**, *36*, 1879–1895. [CrossRef]
62. Breault, R.F.; Smith, K.P.; Sorenson, J.R. *Residential street-dirt accumulation rates and chemical composition, and removal efficiencies by mechanical-and vacuum-type sweepers. New Bedford, Massachusetts, 2003–2004*; US Department of the Interior, US Geological Survey: Reston, VA, USA, 2005; Volume 4.
63. Cristina, C.M.; Sansalone, J.J. "First flush," power law and particle separation diagrams for urban storm-water suspended particulates. *J. Environ. Eng.* **2003**, *129*, 298–307. [CrossRef]
64. Marchioni, M.; Becciu, G. Permeable pavement used on sustainable drainage systems (SUDs): A synthetic review of recent literature. *WIT Trans. Built Environ.* **2014**, *139*, 183–194.
65. Ahmad, K.A.; Abdullah, M.E.; Abdul Hassan, N.; Daura, H.A.; Ambak, K. A review of using porous asphalt pavement as an alternative to conventional pavement in stormwater treatment. *World J. Eng.* **2017**, *14*, 355–362. [CrossRef]
66. Razzaghmanesh, M.; Beecham, S. A review of permeable pavement clogging investigations and recommended maintenance regimes. *Water* **2018**, *10*, 337. [CrossRef]
67. Cristina, C.; Tramonte, J.; Sansalone, J.J. A granulometry-based selection methodology for separation of traffic-generated particles in urban highway snowmelt runoff. *Water Air Soil Pollut.* **2002**, *136*, 33–53. [CrossRef]
68. Allen, T. *Particle Size Measurement*, 2nd ed.; Chapman and Hall: London, UK, 1977.
69. Sansalone, J.J.; Koran, J.M.; Smithson, J.A.; Buchberger, S.G. Physical characteristics of urban roadway solids transported during rain events. *J. Environ. Eng.* **1998**, *124*, 427–440. [CrossRef]
70. Kim, J.Y.; Sansalone, J.J. Event-based size distributions of particulate matter transported during urban rainfall-runoff events. *Water Res.* **2008**, *42*, 2756–2768. [CrossRef] [PubMed]
71. Bader, H. The hyperbolic distribution of particle sizes. *J. Geophys. Res.* **1970**, *75*, 2822–2830. [CrossRef]
72. Lin, H.; Ying, G.; Sansalone, J. Granulometry of non-colloidal particulate matter transported by urban runoff. *Water Air Soil Pollut.* **2009**, *198*, 269–284. [CrossRef]
73. Zhao, H.; Li, X.; Wang, X.; Tian, D. Grain size distribution of road-deposited sediment and its contribution to heavy metal pollution in urban runoff in Beijing, China. *J. Hazard. Mater.* **2010**, *183*, 203–210. [CrossRef] [PubMed]
74. Nichols, P.W.; Lucke, T. A detailed analysis of sediment particle sizes and clogging in permeable pavements. *CLEAN–Soil Air Water* **2017**, *45*, 1700078. [CrossRef]